Comments on "Pore-Scale Visulization of Colloid Transport and Retention in Partly Saturated Porous Media"

Jiamin Wan and Tetsu K. Tokunaga

Lawrence Berkeley National Laboratory

Berkeley, CA 94720

jmwan@lbl.gov

The recent study by Crist et al. (2004) attempted to provide pore scale insights into mechanisms responsible for controlling colloid transport in unsaturated porous media. However, because they relied on images obtained along surfaces that were open to the atmosphere, artificial evaporation resulted in 2 more critical artifacts; formation of air-water-solid (AWS) contact lines, and advection/deposition of colloids to AWS contact lines. These evaporation-related artifacts need to be addressed because they account for most of the colloid deposition at AWS contact lines reported in Crist et al. (2004). . . As stated in Crist el al. (2004), "… the front panel was removed to avoid light reflections that obscured the view and, thus, exposed one side of the sand column to air". Although a more recent paper (Crist et al., 2005) also presents results using the same methods and is therefore also affected by evaporation, we will restrict our present comments to Crist et al. (2004). Here, we show that removal of the front panel results in a sequence of three critical artifacts; (1) significant evaporation, (2) drying of thin films and formation of air-water-solid (AWS) contact lines, and (3) advection of colloids to AWS contact lines where they are deposited. As explained below, these artifacts so drastically disturbed their

system that the magnitude of their observations are not likely to occur anywhere except within the most superficial few cm of soils.

Before explaining these artifacts, we note that although trapping of colloids at AWS contact lines reported in Crist et al. (2004) is largely an artifact of evaporation, colloid filtration within perimeters of pendular rings is in fact a main prediction of the film straining model (Wan and Tokunaga, 1997). In that model, colloid filtration is predicted to be more efficient below a critical water saturation, when capillary connections between pendular rings become separated by adsorbed water films. In that paper we stated that "Retardation of ideal, nonsorbing colloids can occur at two locations: trapped within individual pendular rings due to exclusion from entry into surrounding thin films and within films…" (Wan and Tokunaga, 1997). Thus, while Crist et al. (2004) implied that the film straining model applies only to retardation of colloid transport within thin films, colloid retention within perimeters of pendular rings is a main feature of our model.

Significance of evaporation

In order to determine the significance of evaporation, we constructed a flow chamber having the dimensions presented in Crist et al. (2004), and repeated their wetting and drainage procedures, with and without covering the sand pack. Our tests were conducted on acid-washed Unimin sand of the same grain-size (0.43 to 0.60 mm), at room temperature (21.5˚ to 23.5˚C), under relative humidity (RH) values ranging from 24% to 40%, without lighting or heating from an illuminating device other than ordinary fluorescent lights along the laboratory ceiling. Our tests on covered sand packs were conducted in the manner described in Crist et al. (2004), except that the cover plate remained on until the time at which moisture content sampling was

performed. The air phase in the upper portion of the covered flow chamber was vented to atmospheric pressure via a pair of syringe needles. Like Crist et al. (2004), outflow was undetectable in all of our tests beyond a few minutes after setting the sand at 35˚ inclination angle. However, in open systems such as that used in Crist et al. (2004), hydrostatic conditions cannot be assumed simply because of undetectable drainage. Various moisture profiles obtained in our tests, as well as the profile at 2 hours drainage reported in Crist et al. (2004, estimated from Figure 2 of their paper) are shown in Figure 1. The moisture profiles obtained in our open system at 2 hours of drainage are in rough agreement with Crist et al. (2004), although they obtained drier sands through most of their profiles (40 to 170 mm distances from the top) and slightly wetter sands within the upper section (0 to 40 mm distances). Their generally lower water contents may be a result of additional heating from their lighting system (page 62 of Crist, 2002). In contrast to the moisture profiles obtained from open flow chambers, those obtained on the covered sands remained nearly saturated even in the upper sections. Water contents in the upper region (down to the 70 mm depth along the 35˚ incline) of our open system were clearly much drier than in our covered system. The water loss from the flow chamber during the 2 hour period (shaded area between curves in Fig. 1) normalized to the open sand area is equivalent to an evaporation rate of 83 ±7 μm $hour^{-1}$. Pan evaporation rates of 82 to 120 μm $hour^{-1}$ were measured in the laboratory adjacent to the flow chamber during these experiments. The profile resulting from 11 hours exposure of the sand surface further illustrates the impact of evaporative water loss. Evaporation significantly disturbed moisture contents during and after the 2 hour time frame used for obtaining images, and the assumption made by Crist et al. (2004) that after 2 hours "The moisture content did not vary significantly thereafter, as the drainage from the bottom of the column was minimal to undetectable." was incorrect. While the disturbance was

obvious in these "bulk" measurements obtained on the full 5 mm thickness of the slab sections, artifacts from drying had to be much more severe along the surficial monolayer of sand grains where evaporation took place. Advancement of the drying front downward from this open boundary amplified the magnitude of the evaporation artifact because all of the photographic images were obtained within micrometers of this surface layer.

Air-water-solid contact lines are artifacts caused by evaporation

"AWS interfaces" appear throughout Crist et al. (2004), and are central to their results. However, because dry air-solid interfaces need to be present for AWS contact lines to exist, the significance of such boundaries in most vadose zone environments is questionable. Below depths of a few centimeters, RH values in soils are typically higher than 95% so that thin water films coat surfaces of mineral grains lacking hydrophobic organic coatings. The development of AWS interfaces in experiments of Crist et al. (2004) are problematic because the sands they used (ours as well) were thoroughly acid washed, resulting in strongly hydrophilic (water-wetting) grain surfaces. In the absence of evaporation, no air-solid surfaces or AWS contact lines should exist in their experiments, not even at the lowest volumetric water content of 0.16 (water saturation of 43%). As illustrated in Figure 2a, in partially saturated systems without evaporation, water films coat sections of grain surfaces that are not directly covered by pendular rings or saturated pores. There are no AWS contact lines in partially saturated, hydrophilic porous media. However, in open systems, top surfaces of the uppermost grains are left dry by evaporation, leaving AWS contact lines at boundaries between wet and dry surfaces as illustrated in Figure 2b. Note that in plan view, these AWS contact lines form rings around dry upper surfaces of grains. Because only this uppermost layer of sand grains was observable in Crist et al.

(2004), their images were nearly all affected by artificially generated AWS contact lines. The few images that might have not contained AWS contact lines would have been associated with their highest water saturation locations, e.g., the 18 and 16 cm depths in Figure 5 of Crist et al. (2004).

Colloid accumulation at the AWS contact lines is an artifact of evaporation

Having established the importance of evaporation and the generation of AWS contact lines in the Crist et al. (2004) experiments, we now explain why these artifacts severely altered colloid distributions within the exposed viewing surface. The simplest system in which colloid transport to AWS contact lines can be understood is that of evaporating droplets in contact with flat solid surfaces. Upon evaporation of droplets of solutions and suspensions, a residual ring of precipitated solutes and colloids is deposited immediately adjacent to the original AWS contact line. This is a ubiquitous phenomenon, observed in many familiar situations such as ring stains left behind by dried drops of saline water, coffee, and dilute paints. An excellent review of this phenomenon, theoretical analysis, and experimental tests are presented in Deegan et al. (2000). In brief, a component of advection toward a pinned (stationary) AWS contact line is needed to replenish the perimeter of the evaporating wetted area and keep this region with thinnest water coverage from drying (Fig. 2). Net advection towards the perimeter causes accumulation of solutes and colloids at and near contact lines. Many of the microphotographs presented in Crist et al. (2004) illustrated results of this process. No other mechanism could explain the strong advection of colloids to contact lines, especially after inflow and outflow ceased.

Advection toward AWS contact lines is most clearly observed through microscopy of evaporating droplets of colloidal suspensions (Fig. 3). For this demonstration, a suspension of hydrophilic latex microspheres was prepared in a manner similar to that of Crist et al., 2004 ($\approx 10^8$ particles mL^{-1}, in 0.1 mM $CaCl_2$, pH 5.6). In our test, 1.0 μm Fluoresbrite carboxylate YG microspheres (PolySciences, Inc.) were used. Approximately 1 μL droplets of these suspensions were transferred onto clean glass microscope slides. Droplets were either covered with an inverted cap containing water-saturated filter paper in order to maintain nearly 100% RH in the headspace, or left open to evaporate in the laboratory atmosphere (31% RH). Images of colloid distributions within these droplets were obtained with a Zeiss Axioskop 20 at 100X and 400X magnification (fluorescence illuminated through a 450-490 nm excitation filter). The capped-humidified droplets were uncapped after various equilibration times (20 to 40 minutes), and quickly placed under the microscope. No accumulation of colloids at droplet perimeters (AWS contact lines) was detectable in these capped-humidified systems upon initial viewing. However, colloids were observed to quickly move to stationary AWS lines and deposit in monolayer rings and later into multilayer rings. As shown in Figure 3, colloid enrichment along the contact line was observed within less than a minute of evaporation.

These contrasts in colloid distributions without and with evaporation are also easily observed in the Crist et al. (2004) flow cell. For our visualization test, the flow cell was initially covered, presaturated, and drained as described earlier, but now with a 2 mm spacer so that the window was not in direct contact with the wet sand. The covered flow cell was then transferred onto the microscope stage inclined at 35˚. The suspension of Fluoresbrite microspheres just described was injected following the Crist et al. (2004) procedure, and allowed to drain for 27 minutes with the window still in place to suppress evaporation. The window was then removed

and microphotographs were taken (Figure 4). During the first few minutes, no distinct lines of colloid accumulation were detectable anywhere within the system, consistent with the fact that water contents were high when evaporation was just beginning to have an effect. After about 5 minutes, progressive accumulation of colloids in ring patterns around upper regions of sand grains occurred. The experiments described here are simple to do, and we encourage those interested to perform independent tests of their own.

Acknowledgments

This work was carried out under U.S. Dept. of Energy Contract No. DE-AC03-76SF00098, with funding provided by the U.S. Dept. of Energy, Basic Energy Sciences, Geosciences Research Program.

References

Crist, J. T. 2002. Pore-scale characterization of colloid transport in the unsaturated zone. Ph.D. dissertation, Cornell University.

Crist, J. T., J. F. McCarthy, Y. Zevi, P. Baveye, J. A. Throop, and T. S. Steenhuis. 2004. Pore-scale visualization of colloid transport and retention in partly saturated porous media. Vadose Zone J. 3:444-450.

Crist, J. T., Y. Zevi, J. F. McCarthy, J. A. Throop, and T. Steenhuis. 2005. Transport and retention mechanisms of colloids in partially saturated porous media. Vadose Zone J. 4:184-195.

Deegan, R. D., Bakajian, O., T. F. Dupont, G. Huber, S. R. Nagel, and T. A. Witten. 2000. Contact line deposits in an evaporating drop. Phys. Rev. E 62:756-765.

Wan, J., and T. K. Tokunaga. 1997. Film straining of colloids in unsaturated porous media: Conceptual model and experimental testing. Environ. Sci. Technol. 31:2413-2420.

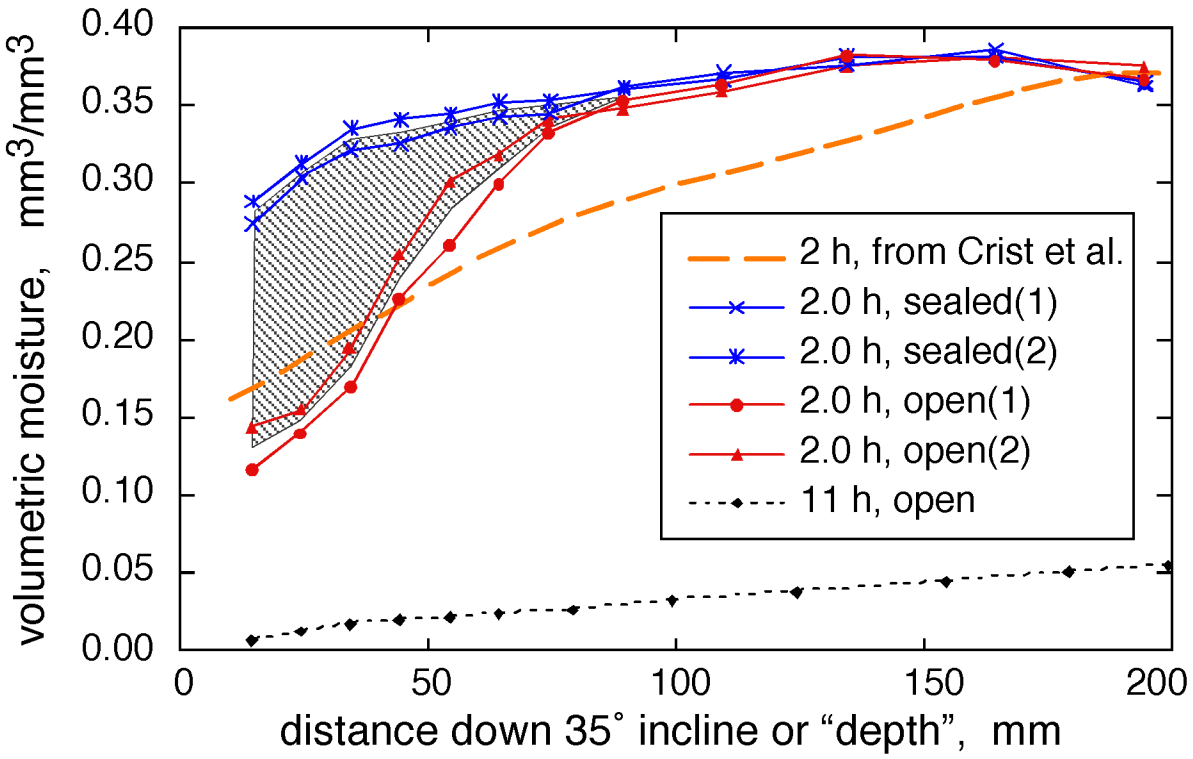

Figure 1. Moisture profiles obtained in seal (pinhole-vented to atmospheric pressure) versus open infiltration chambers. The shaded area indicates the magnitude of bulk water lost by evaporation over a 2 hour period.

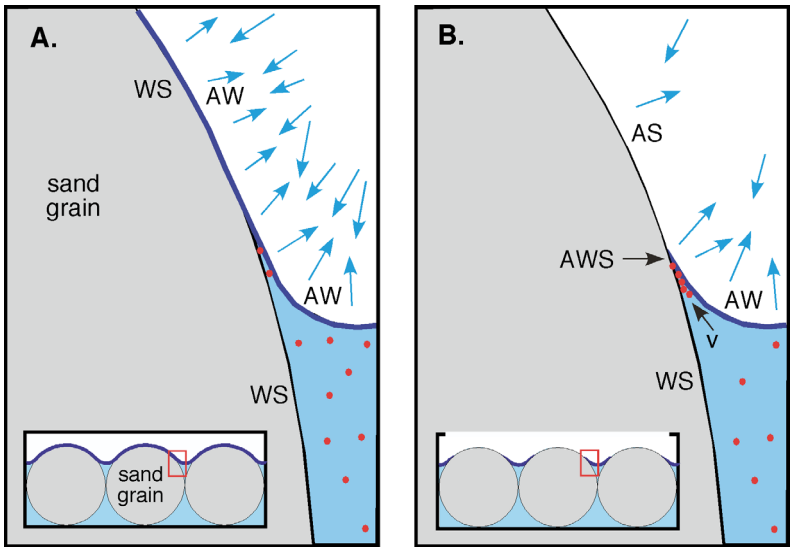

Figure 2. Comparisons between colloid distributions in pendular rings on hydrophilic sand grains (**a**) without, and (**b**) with evaporation. The larger pictures represent enlargements of the boxed region in inserts. Air-water, water-solid, and air-solid interfaces are denoted by AW, WS, and AS, respectively. When local equilibrium exists between capillary/adsorbed water and water vapor in the soil gas phase, no net water loss (evaporation) occurs along AW interfaces. This dynamic equilibrium between evaporation and condensation, depicted by equal number of blue arrows leaving and entering the AW interface in (**a**) and dry (less than monolayer coverage) AS interface in (**b**). Both AS interfaces and the AWS contact lines exist only in systems with net evaporation. While film straining of occurs where pendular rings transition into adsorbed water films (**a**), net water flow (denoted by v) and colloid transport to AWS contact lines occur only in evaporating systems (**b**) where the film straining effect is greatly amplified.

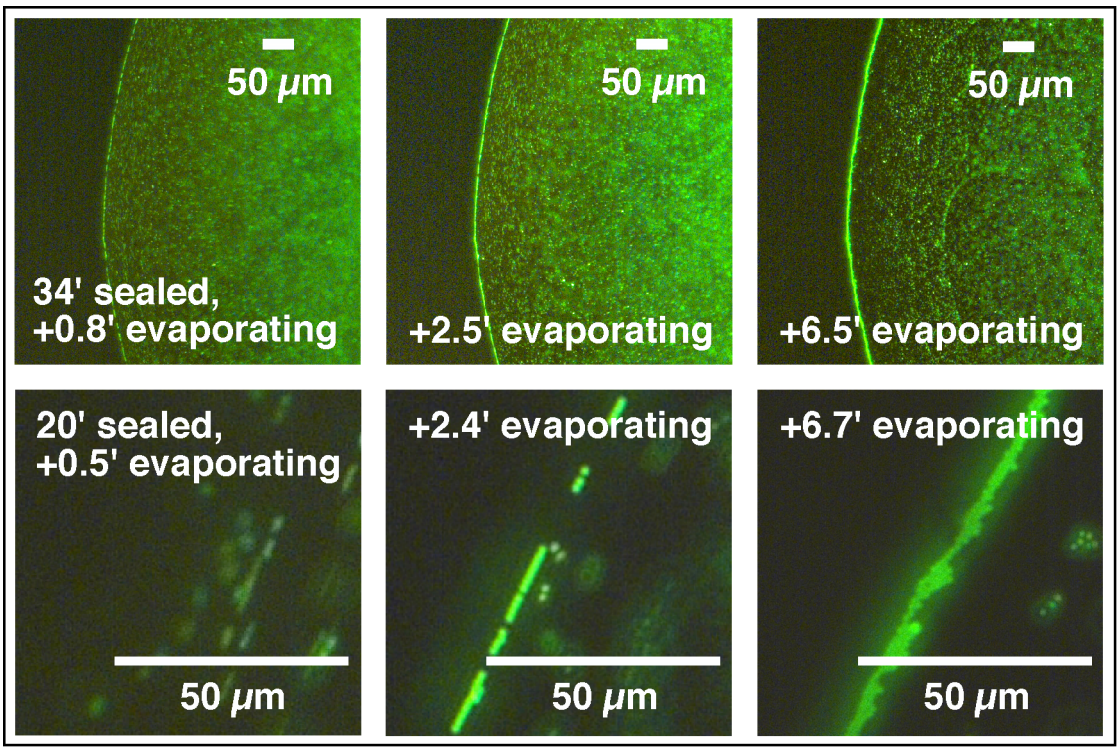

Figure 3. Microphotographs of latex microsphere distributions in the vicinity of AWS contact lines formed upon placing droplets on glass slides. The top row shows a time series of images obtained from a droplet initially maintained in a high humidity atmosphere for 34 minutes, then open to evaporation and photographed (100x) at 0.8, 2,5, and 6.5 minutes of evaporation. The bottom row shows a similar time series, except that the suppressed evaporation period was 20 minutes, and magnification was 400x.

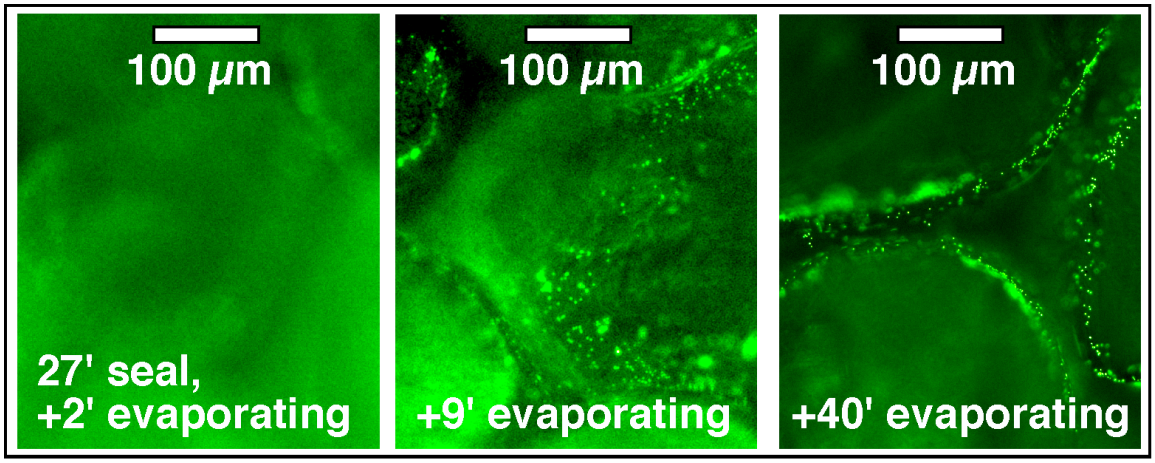

Figure 4. Microphotographs of latex microsphere distributions around sand grains along the viewing surface at 20 mm "depth".